ELSEVIER

Polymer 43 (2002) 3627–3633

polymer

www.elsevier.com/locate/polymer

Molecular mobility in polymers studied with thermally stimulated recovery. II. Study of the glass transition of a semicrystalline PET and comparison with DSC and DMA results

N.M. Alves[a], J.F. Mano[a,*], J.L. Gómez Ribelles[b]

[a]*Department of Polymer Engineering, University of Minho, Campus of Azurém, 4800-058 Guimarães, Portugal*
[b]*Department of Applied Thermodynamics, Center for Biomaterials, Universidad Politécnica de Valencia, P.O. Box 22012, E-46071 Valencia, Spain*

Received 25 June 2001; received in revised form 13 December 2001; accepted 22 February 2002

Abstract

The glass transition of a semicrystalline PET is studied by dynamic mechanical analysis (DMA) and thermally stimulated recovery (TSR). The DMA results allowed us to construct a master curve for E' and D', where the shift factors were modelled with the Vogel–Fulcher–Tamman–Hesse (VFTH) equation above T_g. Using the thermal sampling procedure, the TSR technique allowed us to decompose the complex distribution of retardation times into a set of quasi-elementary processes. At the compensation point a broad distribution of retardation times is observed using DSC data. The TSR results show a typical increase of the activation energies in the glassy state, followed by a decrease above T_g that may be modelled with the VFTH equation. This observation was explained taking into account both the typical time scale range of TS experiments and the evolution of the retardation times distribution with temperatures below and above T_g, under the Adams–Gibbs theory. The evolution of the activation energies from the TSR results was shown to be compatible with the DMA and DSC data.

Keywords: Thermally stimulated recovery; Dynamic mechanical analysis; Viscoelastic behaviour

1. Introduction

The glass transition is the freezing of a supercooled liquid into an amorphous solid. When a liquid is continuously cooled, the rate of diffusion decreases while the viscosity increases, due to a diminishing molecular mobility. The departure from the equilibrium of the material, which is assigned to the formation of the glassy state, depends upon the time scale of the experiment, as well as on the conformational dynamics of the polymeric segments. Therefore the glass transition is observed to be a kinetic phenomenon under typical experimental conditions. The study of the features of polymers near their glass transition is important both for fundamental understanding and for their use in various applications. In fact, the formation of the glassy state results in changes in numerous characteristics including mechanical, dielectric, optical and barrier properties.

Several spectroscopic techniques have been used to study the dynamics of the glass transition, including dielectric, mechanical, NMR and calorimetric analysis [1–4]. Thermally stimulated techniques, such as thermally stimulated depolarisation currents (TSDC) or thermally stimulated recovery (TSR), are transient-like techniques that allow for the investigation of the conformational mobility with a low equivalent frequency [5–10]. TSDC probes essentially the dipolar relaxation and TSR is more sensitive to structural motions that lead to geometrical changes in the sample. By using a specific experimental protocol (thermal sampling, TS, or thermal windowing), thermally stimulated techniques are able to decompose a complex process, characterised by a distribution of characteristic times, into its quasi-elementary components, enabling the analysis of the fine structure of the global spectra [11].

In the previous paper of this series it was demonstrated that TSR experiments can be performed in a conventional dynamic mechanical analyser [12]. This possibility will be explored in this work for the study of the glass transition of a semicrystalline poly(ethylene terephthalate) (PET), enabling a complementary analysis of the data obtained from dynamic mechanical spectroscopy and thermally stimulated experiments. The possibility of comparing the results obtained with these techniques in experiments

* Corresponding author. Tel.: +351-5360-4451; fax: +351-2535-10249.
E-mail address: jmano@dep.uminho.pt (J.F. Mano).

0032-3861/02/$ - see front matter
PII: S0032-3861(02)00176-3

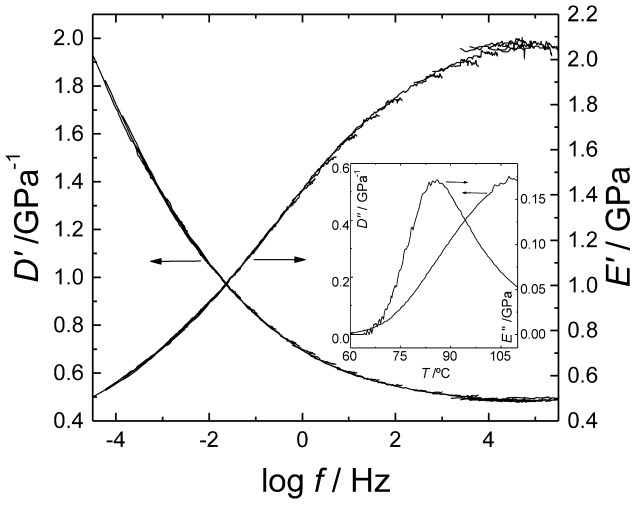

Fig. 1. Master curves of the studied PET sample for the storage modulus (E') and storage compliance (D') constructed from isothermal curves carried out from 51.6 to 103.8 °C. Inset graphics: isochronal result (f = 1 Hz) showing the loss modulus and loss compliance (E'' and D'', respectively).

performed on samples tested under the same conditions (for instance, the same stress mode, thermal environment, geometry,…) allows for a deeper insight in the study of the mechanical behaviour of polymeric materials. The glass transition studied by differential scanning calorimetry (DSC) on the same material will be also compared with the mechanical data, in order to observe how the conformational mobility within the polymeric chains changes with the type of excitation used to investigate the conformational mobility of the polymer chains.

2. Experimental

The studied material was PET, supplied by Goodfellow—catalogue number ES3030310. The sample, in a form of a bar with 1 mm thickness, was kept for 1 h at 163 °C to induce crystallinity. In that way no appreciable changes in the microstructure is expected if one works repeatedly with the same sample at temperature below ~160 °C.

Both the dynamic mechanical analysis (DMA) and TSR experiments were carried out in a DMA7e Perkin–Elmer analyser with controlled cooling accessory. Continuous flux of high purity helium (flow rate of ~65 $cm^3\,min^{-1}$) was used to improve heat transfer throughout the sample surroundings during the experiments.

The experiments on the polymer were carried out with the three point bending mode. The sample was placed over a 15-mm bending platform and a 5-mm knife-edge probe tip provided the mechanical excitation.

The DMA experiments were performed in isothermal conditions, at different temperatures, from 51.6 to 103.8 °C every 2 °C. At each temperature the frequency was scanned from 0.6 to 15 Hz. A static stress of 2.4×10^5 Pa and a dynamic stress of 2×10^5 Pa were imposed to the sample in all experiments.

Using the TSR technique one may perform at least two kind of experiments: the TSR global and the thermal sampling (or windowing) experiments. In both types of experiments a static stress, σ_0, is applied during an isothermal period (at creep temperature T_σ) and during a temperature program at constant rate between T_σ and $T_\sigma - \Delta T_w$. Then without any stress the strain is partially recovered during an isothermal period at $T_\sigma - \Delta T_w$ followed by a cooling down to T_0. Finally, the strain is measured, as a function of temperature, during heating at constant rate ($\beta = dT/dt$) up to a temperature well above T_σ. The difference between both experiments is that, in a TSR global experiment $T_\sigma - \Delta T_w = T_0$, whereas in a TS experiment $\Delta T_w \sim 3$ °C and $T_0 \ll T_\sigma$. In all the experiments carried out in this work we used $\beta = 4$ K min^{-1} and for the TS experiments $\Delta T_w = 3$ °C.

In TS experiments the recovery measured during the heating scan is due to the molecular groups that were activated during the application of static stress σ_0, which are those having relaxation times at T_σ around a certain characteristic time τ_σ which depends on the period of time in which the charge is applied. Thus, the TS experiment allows to resolve the complex relaxational spectrum in nearly elementary mechanisms. On the contrary, in the TSR global experiments the complex nature of the relaxation is studied because all the conformational motions with relaxation times around τ_σ between T_σ and T_0 are activated. The ensemble of the TS experiments within the glass transition region gives an overall picture of the processes associated to the relaxation as probed at low frequencies.

3. Results and discussion

3.1. Dynamic mechanical results

The viscoelastic behaviour of the studied PET was investigated by isothermal DMA experiments within the glass transition range. By horizontal shift of the isothermal E' and D' vs. $\log f$ results obtained at different temperatures it was possible to construct the master curves both for the storage modulus, E', and storage compliance, D' (Fig. 1). The shift factors are found to be the same for the two curves.

The shift factors above T_g were successfully described by the WLF equation [13]

$$\log a_T = \log \frac{\tau(T)}{\tau(T^*)} = -\frac{C_1(T - T^*)}{C_2 + (T - T^*)} \quad (1)$$

where a_T is the shift factor, T^* is a reference temperature and C_1 and C_2 depend on the material and on T^*. This expression is usually valid for polymers over the temperature range $T_g < T < T_g + 100$ °C (where T_g is the glass transition temperature) and when T^* is identified with T_g, it was seen that C_1 and C_2 assume 'universal' values close to 17.44 and

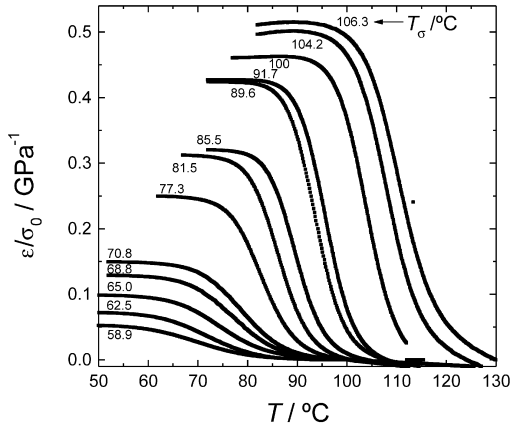

Fig. 2. TS results of the studied PET in the glass transition region, obtained at different creep temperatures, T_σ.

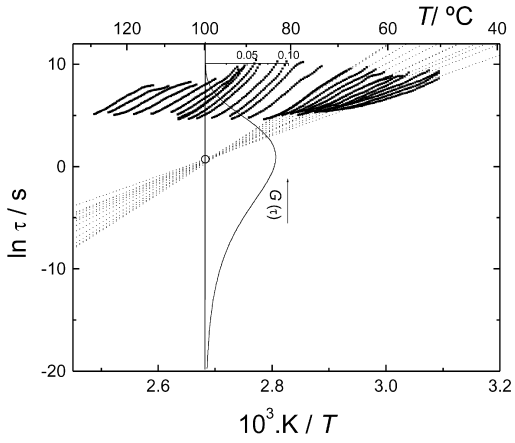

Fig. 3. Solid lines: Arrhenius lines of several TS experiments on the studied PET in the glass transition region. In the glassy state the lines converge (dotted lines) to the compensation point (circle). The distribution of retardation times at the compensation temperature ($T_c = 100$ °C), calculated from DSC data, is shown as a function of log τ using the same axis as for the Arrhenius plot.

51.6 °C, respectively [13]. In a more recent work the determination of C_1 and C_2 in the glass transition zone, on a wide range of polymers, indicated that C_1 may range between 15 and 26 and C_2 between 20 and 130 °C [14]. This description can also be used at temperatures below T_g if the polymer is at its equilibrium density. It is easy to show that Eq. (1) is equivalent to the Vogel–Fulcher–Tamman–Hesse equation (VFTH) [15–17],

$$\tau(T) = \tau_0 \exp\frac{B}{T - T_0} \tag{2}$$

where τ_0 is a pre-exponential factor and B and T_0 are specific adjustable parameters. As commented by Angell [18], τ_0 is seen as a microscopic quantity related to the frequency of attempts to cross some barrier opposing the rearrangement of particles involved in the relaxation [19,20], or the time a molecule needs to move into some free space [21–23]. T_0 is a diverging temperature, implying the physical impossibility of configurational changes in the solid (the configurational entropy, S_c, tends to 0 at that temperature), close to the Kauzmann temperature [24] and BT_0 is a parameter which can be related with the fragility concept first introduced by Angell [25].

The C_1 and C_2 parameters were calculated by a linear regression of $1/\log a_T$ vs. $1/(T - T^*)$ in the viscous liquid phase, using $T^* = 81.3$ °C. The B and T_0 parameters of the VFTH equation can also be directly calculated from the C_1 and C_2 parameters. We observed the same C_1 and C_2 parameters for both E' and D' results: $C_1 = 18.1$ and $C_2 = 71.8$ °C. Those values, that are in agreement with those referred in Ref. [14], lead to the Vogel parameters $B = 2999.7$ K and $T_0 = 11.3$ °C. The pre-exponential factor of the VFTH equation can be known if one accede to any pair of $\tau(T)$. An isochronal experiment performed at $f = 1$ Hz ($\tau = 1/2\pi f = 0.159$ s), shown in the inset of Fig. 1, presented the maximum of E'' and D'' at $T = 82.8$ and 104.4 °C, respectively. The obtained pre-exponential factors are: 2.04×10^{-20} s for the E' results and 1.97×10^{-16} s for the D' results. This allowed, for the first case, to calculate all the VFTH parameters of the relaxation times whereas, for the second case, the same parameters for the retardation times.

3.2. TSR results

The PET sample was studied by TSR using the TS procedure. Some normalised ε vs. T curves obtained in the glass transition region are shown in Fig. 2. The low temperature plateau of the TS curves increases as T_σ increases. This is a typical behaviour of this kind of experiments [26,27]. Similarly, TS results from TSDC experiments in the glassy state, exhibit an increase of the total polarisation with increasing polarisation temperature towards T_g [6,7,28]. The explanation for this behaviour will be given later.

The anelastic response associated to each TS curve is usually analysed as a quasi-elementary process, often modelled by a Debye (for dielectric response) or a Voigt–Kelvin model (for mechanical response). The temperature dependence of the retardation time of such curves are obtained up to near the temperature of maximum strain-rate, using the so-called Bucci method (see details in the first part of the work [12])

$$\tau(T) = \frac{1}{\beta}\frac{\varepsilon(T)}{|\mathrm{d}\varepsilon(T)/\mathrm{d}T|} \tag{3}$$

where β is the heating rate. The relaxation map for some TS results in the studied PET is shown in Fig. 3. The characteristic times range between 100 s (near the temperature of maximum strain-rate) and 10 000 s, which are comparatively high if one takes the reciprocal frequencies usually employed in dynamic spectroscopic techniques. Due to the narrow characteristic time range observed in the TS relaxation map, the Arrhenius equation is usually used to fit the data, allowing to obtain both the activation energy, E_a, and

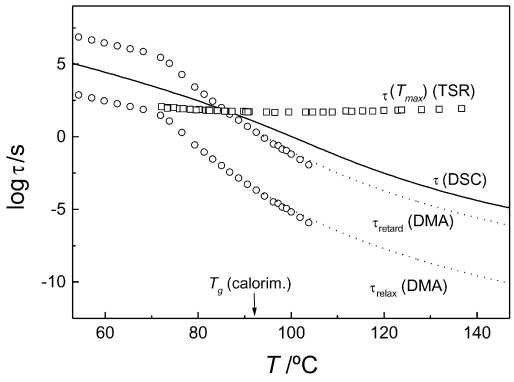

Fig. 4. Squares: retardation time at the inflexion temperature of the TS curves (T_{max}) as a function of T_{max} for the studied PET. Circles: mean characteristic times as a function of temperature calculated from the master curve of E' (relaxation times, τ_{relax}) and calculated from the master curve of D' (retardation times, τ_{retard}); the dotted lines linked to these data are extrapolations to higher temperatures according to the VFTH equation. Solid line: mean retardation times as a function of temperature for a DSC experiment on cooling at 40 °C min^{-1} [31].

the pre-exponential factor, τ_0 of each TS curve

$$\tau(T) = \tau_0 \exp\frac{E_a}{RT} \tag{4}$$

where R is the perfect constant gas. The dotted lines in Fig. 3 are the Arrhenius fittings of the TS data obtained at T_σ below T_g. As often reported, the Arrhenius lines of the TS curves obtained in the glass transition region but below T_g tend to converge in a single point, the compensation point characterised by a compensation temperature (T_c) and a compensation time (τ_c). This compensation phenomenon can be seen by the almost perfect linear relationship between the activation energies and pre-exponential factors of the different TS curves. The compensation parameters can be obtained from a fitting of such kind of plot [27]. For the case of the studied PET, we obtained $T_c = 100$ °C and $\tau_c = 2$ s. Although this compensation effect has been extensively discussed in the literature [29,30] an unambiguous consensus about its physical origin was not yet achieved.

An important feature of the compensation effect is that it predicts that all individual processes in the glassy state that would be involved in the glass transition should have the same characteristic time at the compensation temperature.

Complementary data of the glass transition dynamics of the studied material, obtained by DSC, could be used for the determination of the distribution of characteristic times at T_c. The DSC results of this material obtained with different thermal histories were analysed using a phenomenological model based on configurational entropy concepts [31]. This model is a modification of the Scherer–Hodge model [32,33] and has the advantage of avoiding the calculation of the fictive temperature, which needs a previous assumption for the form of the temperature dependence of the configurational heat capacity with temperature. It was then possible to calculate the temperature dependence of τ and the exponent of the KWW stretched-exponential decay function [34,35], β, that gives information of the distribution of characteristic times. The distribution function $G(\tau)$ associated with the KWW model, can be calculated numerically using [36]

$$G(\tau) = -\frac{\tau_{kww}}{\pi\tau}\sum_{k=0}^{\infty}\frac{(-1)^k}{k!}\sin(\pi\beta k)\Gamma(\beta k+1)\left(\frac{\tau_{kww}}{\tau}\right)^{\beta k+1} \tag{5}$$

where τ_{kww} is the characteristic time of the KWW model and $\Gamma(x)$ is the gamma function. Using $\tau_{kww}(T_c = 100\,°C) = 1.1$ s and $\beta = 0.22$, extracted for Ref. [31], it was possible to compute the distribution of characteristic times at the compensation temperature using Eq. (5). This distribution function is shown in Fig. 3. It is clear that at $T = T_c$ a broad distribution of characteristic times exists. This disclaims a genuine physical meaning of the compensation phenomenon, that predicts a single retardation time at T_c. Thus, the compensation effect seems to be associated to a consequence of some intrinsic features of the technique.

3.3. Temperature dependence of the characteristic times and activation energies

The values of τ calculated with Eq. (3) at the temperature of maximum strain-rate, T_{max}, is often a measure of the time scale of TS experiments due to the fact that at that temperature the variation of the strain during the recovery process is maximum. Fig. 4 show $\tau(T_{max})$ as a function of T_{max} for the different TS curves (squares). The retardation times do not vary significantly in the logarithmic axis, taking values near 10^2 s, like as in TSDC data [37]. Such values are also typical for DSC time scales.

During TSR experiments we measure a strain at zero stress, i.e. the intrinsic response of the system has a character of susceptibility. Thus, the characteristic times associated with the TSR techniques are retardation times. Therefore the dynamic viscoelastic parameter that could be compared with the TSR results and that reflex such characteristic times, is the compliance ($D^* = D' - iD''$).

From the previous DMA results we can plot the temperature dependence of the mean retardation (from the D' data) and relaxation (from the E' data) times in the studied temperature range (Fig. 4). The DMA data in the equilibrium region were fitted according to the VFTH equation and the corresponding extrapolations of the characteristic times were extended to higher temperatures in Fig. 4 (dotted lines). Note that DMA data in Fig. 4 are, in nature, different from the TSR one. The former are assigned to the mean characteristic times at each temperature and the later are related with the temperature dependence of specific modes (from the distribution of retardation times associated to the glass transition) probed at approximately the same time scale (10^2 s).

Fig. 4 also show the mean retardation times calculated

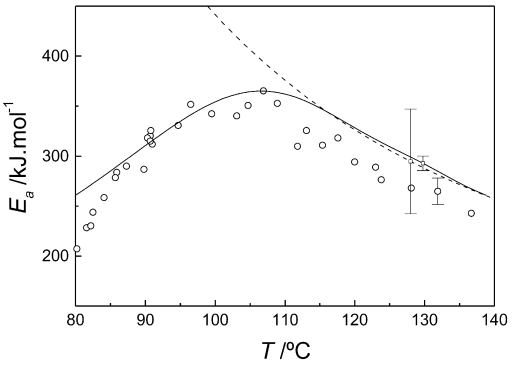

Fig. 5. Activation energies as a function of temperature calculated in both the glassy and equilibrium states from TS (circles) and from DSC experiments (solid line). The dashed line is the activation energy calculated from the DMA results in the equilibrium state, using the VFTH equation. The error in the TS data is assumed to be below 10% [12] and it was found that in DSC the error in the activation energy when one used the method proposed should be around 5% [44]. The errors in the DMA line were obtained from the errors of the fitting with the WLF equation.

from DSC experiments using a modelling procedure, previously described [31]. Above T_g such data can be compared with the retardation times obtained by DMA. It can be seen in Fig. 4 that the lines are quite parallel being the DSC times higher than the DMA ones. In fact the same physical phenomenon is analysed, which is assigned to the conformation rearrangements in the glass transition region. Therefore, the change of the dynamics with temperature should be probed similarly by both techniques. Nevertheless, the type of solicitation and the measured properties are distinct. Thus the DSC and DMA times at a given temperature should not be necessarily equal. It should be noted that in the glassy state the direct comparison between the DSC and DMA data can no longer be valid due to the fact that both experiments are performed under very distinct thermal histories. The DSC curve corresponds to a cooling experiment at 40 °C min^{-1} whereas the DMA data results from isothermal experiments, where the sample stayed ~20 min at each temperature.

The DSC data covers a temperature range that goes from the glassy state up to the equilibrium phase. Below T_g (≈92 °C) a typical Arrhenius-like behaviour is detected from the linearity between log τ and $1/T$. Above T_g the VFTH model describes well with the results [31]. This behaviour is also observed with the DMA data (Fig. 4).

Some theories have been able to account for the VFTH equation. For example, the work of Adams and Gibbs [19] enabled to relate the mean structural relaxation time with the temperature and the configurational entropy

$$\tau = \tau_0 \exp \frac{N_A s_c^* \Delta\mu}{k_B T S_c} \tag{6}$$

where N_A is the Avogadro's number, s_c^* is the entropy of the minimum number of particles able to rearrange cooperatively, $\Delta\mu$ is the activation energy per particle opposing a cooperative rearrangement of the liquid/glass structure, k_B is the Boltzmann constant, and τ_0 is the reciprocal of an attempt frequency, similarly to the one in Eq. (2). The temperature dependence of S_c may be calculated from the configurational heat capacity, ΔC_p

$$S_c(T) = \int_{T_0}^{T} \frac{\Delta C_p}{T'} dT' \tag{7}$$

Considering in a simple approach, ΔC_p to be proportional to $1/T$ [38] one may write

$$\Delta C_p(T) = \Delta C_p(T_g) T_g / T. \tag{8}$$

As the heat capacity discontinuity at T_g arises mostly from configurational contributions we may use this expression in the integral of Eq. (7):

$$S_c(T) = T_g \Delta C_p(T_g) \frac{T - T_0}{T T_0} \tag{9}$$

The substitution of Eq. (9) in Eq. (6) can lead to the VFTH formula with $B = N_A s_c^* \Delta\mu T_0 / k_B T_g \Delta C_p(T_g)$.

The theory of Adams and Gibbs is also appropriate to describe the evolution of the relaxation time throughout the glassy state. When the freezing of the cooperative mobility become visible upon cooling, near T_g, the configurational entropy tends to be constant and Eq. (6) takes the Arrhenius equation with apparent activation energy $N_A s_c^* \Delta\mu / S_c$. Therefore the Adams and Gibbs theory explains the change from the VFTH to the Arrhenius regime that is seen in Fig. 4 for the DSC curve. At temperatures above the glass transition temperature, the apparent activation energy, $E_a = R\, \mathrm{d}(\ln \tau)/\mathrm{d}(1/T)$, increases as the temperature decreases according to the VFTH equation:

$$E_a(T) = \frac{RBT^2}{(T - T_0)^2} \tag{10}$$

The apparent activation energy of the studied PET obtained by DSC, obtained from differentiation of data shown in Fig. 4, is shown in Fig. 5 (solid line). The temperature dependence of E_a goes through a maximum at a temperature around T_g when the change between the Arrhenius and VFTH regimes takes place. This behaviour has been also shown in low-frequency dielectric spectroscopy [39] and TSDC techniques [40].

In this work the dependence of E_a with T_{max}, obtained with the TS technique, will also be analysed. Usually such kind of plots, often presented in classical TSDC and TSR results, is used to extract some information of the studied relaxational process (broadness, maximum energy, cooperativity,…), as can be seen, for example, in Refs. [26,41,42]. Such representation for the results on the semicrystalline PET studied in this work is shown in Fig. 5 (open circles). One observes that the activation energy increases in the glassy state, which is always observed in TSDC and TSR results in the glass transition region. These values can go up to 400–500 kJ mol^{-1}, due to the cooperative character of

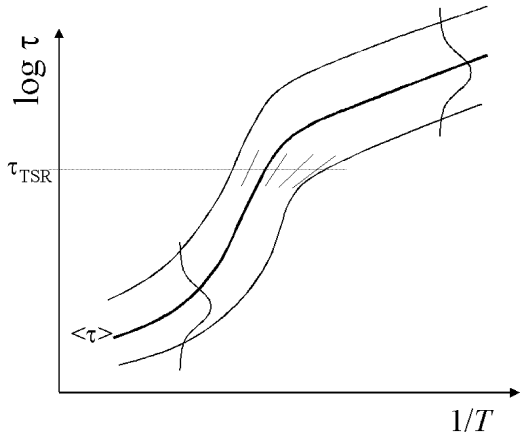

Fig. 6. Typical profile of the distribution of relaxation/retardation times in the glass transition region. The thick line represents the logarithm of the mean characteristic time against $1/T$. The thinner lines correspond to a measure of the envelope of the distribution of characteristic times. Some Arrhenius lines that could be obtained from TS experiments are shown for the typical frequency range associated with the TSR technique, τ_{TST}.

the conformational rearrangements within the macromolecular segments. However, above a temperature around T_g the activation energy starts to decrease continuously with increasing temperature. These tendencies for the E_a path was also observable by TSDC in different systems (e.g. [41–43]). An explanation for that behaviour will be given now.

In order to simplify the discussion we will consider a thermorheologically simple system, i.e. a system in which all the molecular mechanisms contributing to the time and frequency dependent modulus and compliance functions have the same temperature dependence. A typical relaxation map of this system, in its glass transition region, is shown in Fig. 6. The thicker line represents the mean characteristic time as a function of reciprocal of temperature. Two lines follow this thick line in both the up and down sides and essay to represent the edges of the distribution for each temperature at a certain level; for example, at a given temperature, 90% of the retardation times are included between these two lines. An hypothesis of such distribution of retardation times is shown as a vertical bell-shaped curve at two different temperatures, in the glassy and equilibrated states. Fig. 6 shows the dynamic behaviour at temperatures above T_g, with the typical VFTH behaviour, and the progress to an Arrhenius response when the temperature decreases in the direction of the glassy state.

Some typical straight Arrhenius lines, obtained from TS experiments at different T_σ (as those of Fig. 3), are shown schematically in Fig. 6. When one performs TS experiments at a given creep temperature, T_σ, the strain recovery of the activated species are monitored during the final heating. Such species are the ones that at temperatures around T_σ have retardation times of the order of $\tau_{TSR} \sim 10^2$ s.

For low T_σ (experiments in the glassy state) the apparent activation energy is close to the activation energy of the glass. When T_σ increases the activation energy increases due to the progress towards the thermodynamic equilibrium (see increase of the slope of the Arrhenius lines in Fig. 6). Note that during this increase of T_σ in the glassy state the intensity of the activated modes in a TS experiment increases because one approaches the maximum of the distribution of retardation times, that occurs near T_g. Therefore, an increase of ε_0 is expected (or the total polarization for the case of TSDC experiments) when T_σ increases in the glassy state. This tendency is well observed in Fig. 2.

When T_σ is of the order of the calorimetric T_g, the amorphous fraction of the material is essentially in the equilibrium liquid region and for further increases of T_σ the activation energy continuously decreases. This decrease can be easily understood from Fig. 6: if a retardation time in the equilibrium state is fixed, the apparent activation energy assigned to the components of the distribution of retardation times decreases as the temperature increases. The apparent activation energy in this region may be given by Eq. (10).

An interesting result of this work is that Fig. 5 shows a good agreement between DSC and TSR. It seems that the maximum in E_a that represents the transition from VFTH to Arrhenius regimes occurs at the same temperature in two techniques, that have close equivalent frequencies. The apparent activation energy was also plotted for the DMA results in the equilibrated state ($T > T_g$) calculated with Eq. (10), using the obtained VFTH parameter values. Again in this temperature region, the DMA results are consistent with those obtained with the other two techniques.

The agreement in the results from the three techniques indicates that the change of the characteristic times with temperature is independent, in this case, on the spectroscopic technique used. This agreement should only be possible if the studied system has a thermorheologically simple character. In fact, the frequency range acceded by the TSR technique is fundamentally unchanged and the characteristic times used for the calculation of the activation energy from the DSC and DMA techniques covers a broad range (Fig. 4). It should be added in this context that the TSR technique could be used, in principle, in thermorheologically complex systems. As commented by McCrum [45], it is not a requirement for performing TS experiments that all characteristic times have the same shift factor. What is required is that the narrow packet of stimulated processes (typically 1.5 decades wide, as seen in this work) have the same activation energy within the error of the experiment.

4. Conclusions

Master curves of E' and D' were successfully constructed for a semicrystalline PET in the glass transition region. The Vogel–Fulcher–Tamman–Hesse parameters were obtained from the shift factors. Using the same equipment, it was possible to perform TSR experiments, namely using the

TS protocol. Such experiments enabled to draw Arrhenius lines that showed the typical compensation behaviour. It was shown that at the compensation temperature the retardation times are characterised by a broad distribution.

Above T_g the mechanical retardation times are higher than the calorimetric ones. However, the apparent activation energies agree above T_g for these two techniques. Moreover, the apparent activation energy of the DSC results is in good agreement with the activation energies of the TS data, both in the glassy and rubbery states.

The activation energies increase as the temperature increases up to 105 °C and decreases for higher temperatures. This tendency was explained by looking at the evolution of the distribution of retardation times with temperature, both below and above T_g, and the time scale range of the TS experiments.

Acknowledgements

NMA and JFM acknowledge the financial support of Fundação para a Ciência e Tecnologia (Project PRAXIS/P/CTM/14171/1998). Support from the Portuguese–Spanish joint research action (Spain:HP1999-0024; Portugal:E/69/00) is also acknowledged.

References

[1] Jäckle J. Rep Prog Phys 1986;49:171.
[2] Colmenero J, Alegría A, editors. Basic features of the glassy state. Singapore: World Scientific, 1990.
[3] Seyler R, editor. Assignment of the glass transition. Philadelphia: ASTM Publications, 1994.
[4] Richert R, Blumen A, editors. Disordered effects on relaxational processes. Berlin: Springer, 1994.
[5] van Turnhout J. Thermally stimulated discharge of polymer electrets. Amsterdam: Elsevier, 1975.
[6] Mano JF, Moura Ramos JJ, Fernandes A, Williams G. Polymer 1994;35:5170.
[7] Mano JF, Moura Ramos JJ. J Therm Anal 1995;44:1037.
[8] Diffalah M, Demont Ph, Lacabanne C. Thermochim Acta 1993; 226:33.
[9] Martinez JJ, Lacabanne C. Thermochim Acta 1993;226:51.
[10] Dufresne A, Etienne S, Perez J, Demont P, Diffalah M, Lacabanne C, Martinez JJ. Polymer 1996;37:2359.
[11] Chatain D, Gautier PG, Lacabanne C. J Polym Sci 1973;11:1631.
[12] Alves NM, Mano JF, Gómez Ribelles JL. J Therm Analys Calorim, accepted.
[13] Williams ML, Landel RF, Ferry JD. J Am Ceram Soc 1953;77:3701.
[14] Plazek DJ, Ngai KL. Temperature dependencies of the viscoelastic response of polymeric systems. In: Mark JE, editor. Physical properties of polymers handbook. New York: AIP Press, 1996. Chap. 25.
[15] Vogel H. Phys Z 1921;22:645.
[16] Fulcher GA. J Am Chem Soc 1925;8:339.
[17] Tamman G, Hesse WZ. Anorg Allg Chem 1926;156:245.
[18] Angell CA. Polymer 1997;26:6261.
[19] Adams G, Gibbs JH. J Chem Phys 1965;43:139.
[20] van Danne H, Fripiat JJ. J Chem Phys 1978;62:3365.
[21] Cohen MH, Turnbull D. J Chem Phys 1959;31:1164.
[22] Cohen MH, Grest GS. Phys Rev B 1979;20:1077.
[23] Cohen MH, Grest GS. Adv Chem Phys 1981;48:370.
[24] Kauzmann W. Chem Rev 1948;43:219.
[25] Angell CA. J Non-Cryst Solids 1991;131–133:13.
[26] Alves NM, Mano JF, Gómez Ribelles JL. Macromol Symp 1999; 148:437.
[27] Alves NM, Mano JF, Gómez Ribelles JL. Mater Res Innovat 2001; 4:170.
[28] Mano JF, Correia NT, Moura-Ramos JJ, Andrews SR, Williams G. Liq Cryst 1996;20:201.
[29] Lacabanne C, Lamure A, Teyssedre G, Bernes A, Mourgues M. J Non-Cryst Solids 1994;172–174:884.
[30] Moura-Ramos JJ, Mano JF, Sauer BB. Polymer 1997;38:1081.
[31] Alves NM, Mano JF, Balaguer E, Meseguer Dueñas JM, Gómez Ribelles JL. Polymer 2002, in press.
[32] Scherer GW. J Am Ceram Soc 1984;67:504.
[33] Hodge IM. Macromolecules 1987;20:2897.
[34] Kohlrausch R. Prog Ann Phys 1854;91:179.
[35] Williams G, Watts DC. Trans Faraday Soc 1970;66:80.
[36] Lindsey CP, Patterson GD. J Chem Phys 1980;73:3348.
[37] Mano JF. Thermochim Acta 1999;332:161.
[38] Angell CA, Bressel RD. J Phys Chem 1972;76:3244.
[39] Saito S, Nakajima T. J Appl Polym Sci 1959;2:93.
[40] Mano JF, Alves NM, Meseguer Dueñas JM, Gómez Ribelles JL. Polymer 1999;40:6545.
[41] Doulut S, Demont P, Lacabanne C. Macromolecules 2000;33:3425.
[42] Sauer BB, Kim YH. Macromolecules 1997;30:3323.
[43] Mano JF, Correia NT, Moura Ramos JJ. J Chem Soc Faraday Trans 1995;91:2003.
[44] Saiter A, Oliver JM, Saiter JM, Gómez Ribelles JL. Submitted for publication.
[45] McCrum MG. Polymer 1984;25:309.